


Article

Selection of an Appropriate Pre-Injection Pattern in a Marine Diesel Engine Through a Multiple-Criteria Decision Making Approach

María Isabel Lamas Galdo ^{1,*} , Laura Castro-Santos ¹  and Carlos G. Rodríguez Vidal ²¹ Escola Politécnica Superior, Universidade da Coruña, 15403 Ferrol, Spain; laura.castro.santos@udc.es² Norplan Engineering S.L., 15570 Naron, Spain; c.rodriguez.vidal@udc.es

* Correspondence: isabellamas@udc.es; Tel.: +34-881013896

Received: 18 March 2020; Accepted: 31 March 2020; Published: 4 April 2020



Abstract: In the present work, a numerical model was developed to analyze a commercial diesel engine. The adequacy of this model was validated using experimental results. This model was employed to study several pre-injection strategies. Particularly, the pre-injection rate, duration and starting instant were analyzed in the ranges 5% to 25%, 1° to 5° and −22° to −18°, respectively. The effect on consumption and emissions of NO_x, CO, and HC were evaluated. Since some of these configurations have opposite effects on consumption and/or emissions, it is necessary to develop a formal tool to characterize the most appropriate injection pattern. To this end, a multiple-criteria decision making approach was employed. It was found that the injection duration must remain as low as possible due to significant reductions in NO_x. The most appropriate injection pattern resulted 1° pre-injection duration, 20% pre-injection rate, and −19° pre-injection starting instant. This configuration leads to increments of 6.7% in consumption, 3.47% in CO, and 3.83% in HC but reduces NO_x by 34.67% in comparison with the case without pre-injection.

Keywords: MCDM; CFD; engine; emissions; consumption

1. Introduction

It is well known that diesel engines are efficient thermal machines but emit significant levels of harmful gases such as CO₂, Particulate Matter (PM), NO_x, CO, HC and SO_x [1]. Between these, PM and NO_x are especially important in diesel engines. Smoke emissions, related to PM, mostly composed of soot, are related to several diseases but are not globally regulated [2]. On the other hand, ever increasing NO_x emission limits have been imposed by regional and international authorities [3]. According to this, several procedures have been developed in the recent years to reduce NO_x emissions in diesel engines such as EGR, water injection, modification of the injection parameters and after-treatments [4–7]. Between these measurements, this paper focuses on multiple injection strategies using pilot injections. This strategy affects mixing and combustion [8]. Several works about the advantages and disadvantages of pilot injections can be found in literature. One of the main disadvantages is that soot can increase because pilot injections aggravate spray characteristics and particulates can be formed at the rich region [9,10]. In order to avoid this problem, some authors recommend combining multiple injections with other systems such as EGR [11] or high injection pressures [12], while other researchers indicate that it is possible to obtain both NO_x and particulate reduction using only multiple injections. In this regard, Carlucci et al. [13] analyzed the pilot injection timing and duration and found that NO_x emission levels are mainly influenced by the pilot duration, whereas smoke emission is influenced by both variables. Tanaka et al. [14] analyzed the time and quantity of the pilot injection. Benajes et al. [15] analyzed the effect of the dwelling time, i.e., the time between two consecutive injections, obtaining reductions

in noise, NO_x and particulates. Pierpont et al. [16] varied the fuel distribution in each pulse and the dwelling time between pulses and obtained a reduction in NO_x and particulates but also a 3%–4% increase in consumption. Hotta et al. [17] analyzed the number of pre-injections and obtained reductions in both NO_x and HC. Fang et al. [18] analyzed the effect of the injection angle when using multiple injections. Other works such as those of Ishida et al. [19] and Minani et al. [20] obtained NO_x and consumption reductions but recommended employing a small amount of pilot quantity in order to maintain soot emissions. In addition to these aforementioned works based on diesel engines, other similar studies were realized using biodiesel [21], gasoline [22–24], dual fuel [25–28] and other fuels [29–34].

Numerical simulations also provide interesting information to analyze multiple injections. Particularly, in the field of Computational Fluid Dynamics (CFD), one can refer to the work of Lechner et al. [35], who analyzed advanced injection strategies to achieve partially premixed combustion in a diesel engine; Sun and Reitz [36], who analyzed injection strategies to optimize two-stage combustion; Verbiezen et al. [37], who analyzed the effect of injection timing; Zehni and Jafarmadar [38], who analyzed the effect of split injection in a direct-injection diesel engine; Abdullah et al. [39], who analyzed the effect of injection pressure; Coskun et al. [40], who analyzed second injection timings; Wang et al. [41], who analyzed several fuel injection strategies on a gasoline engine; Zhaojie et al. [42], who analyzed two-stage fuel injection with EGR; Lamas et al. [43,44], who analyzed several configurations of pilot injections; and Sencic [45], who analyzed alternative injection patterns.

Despite this literature about multiple injections, it is important to develop a reliable tool to characterize the most appropriate injection pattern. In this regard, this work presents a Multiple-Criteria Decision Making (MCDM) approach to characterize the most appropriate injection pattern. MCDM methodologies constitute a formal tool to handle complex decision-making situations, providing coherence in the decision process. Three pre-injection parameters such as pre-injection rate (R), duration (D) and starting instant (S) were analyzed. The emissions and consumption analyzed in the present work were obtained through a CFD model previously validated with experimental results.

2. Materials and Methods

The engine analyzed in the present work is the Wärtsilä 6 L 46. This is a four-stroke diesel engine with six cylinders. Each cylinder presents two intake and two exhaust valves. The fuel injector has 10 holes and is placed at the center of the cylinder head. The fuel is injected directly into the cylinder since it is a direct injection engine.

The geometry and mesh were realized using SolidEdge and Gambit softwares, respectively. A grid independence study was carried out to provide its adequacy. The software OpenFOAM was employed for the CFD simulations. OpenFOAM was chosen because it is an open software which allows a complete manipulation of the code. The simulation started at 360° Crank Angle After Top Dead Center (CA ATDC) and the whole cycle was analyzed. As boundary conditions, the heat transfer from the cylinder was modelled as a combined convection–radiation. The RANS (Reynolds-averaged Navier-Stokes) equations of conservation of mass, momentum and energy were solved. The k-ε was employed as the turbulence model due to its robustness and reasonably accuracy for a wide range of turbulent flows. As fuel droplet breakup, the Kelvin–Helmholtz and Rayleigh–Taylor breakup models [46] were employed, and the Dukowicz model [47] for the heat-up and evaporation. Regarding the chemical kinetics, a reaction mechanism was programmed by combining the following three kinetic schemes:

- Ra and Reitz's [48] kinetic scheme, based on 131 reactions and 41 species, for combustion.
- Yang et al.'s [49] kinetic scheme, based on 20 species and 43 reactions, for NO_x formation.
- Miller and Glarborg's [50] kinetic scheme, based on 24 species and 131 reactions, for NO_x reduction.

This numerical model was validated using experimental measurements. For this purpose, experimental measurements obtained elsewhere [51–55] were employed. The emissions and Specific

Fuel Consumption (SFC) obtained numerically and experimentally at several loads are indicated in Figure 1. This figure shows a reasonable correspondence between numerical and experimental results. The in-cylinder pressure obtained numerically and experimentally at 100% load is shown in Figure 2. This figure also shows a satisfactory correspondence between experimental and numerical results. A certain error was inevitable due to both numerical and experimental handicaps. On the one hand, the instruments employed to characterize experimental measurements have a certain tolerance and, on the other hand, numerical errors are introduced due to the discretization processes and the hypothesis assumed to simplify the governing equations.

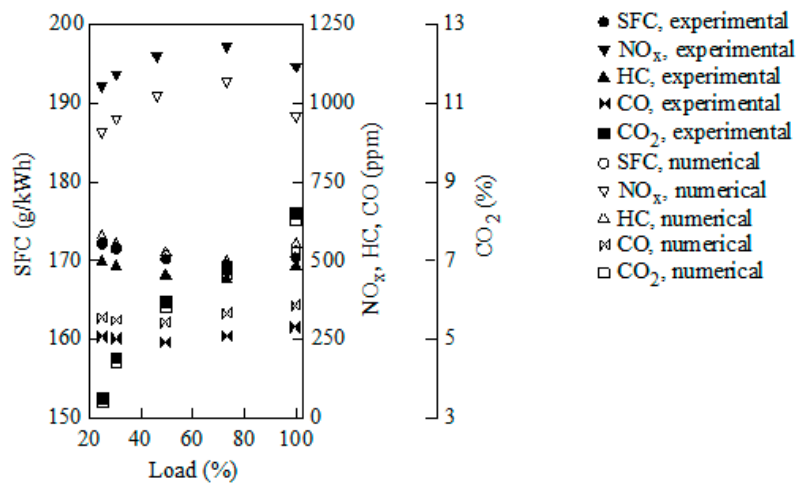


Figure 1. SFC and emissions numerically and experimentally obtained at different loads.

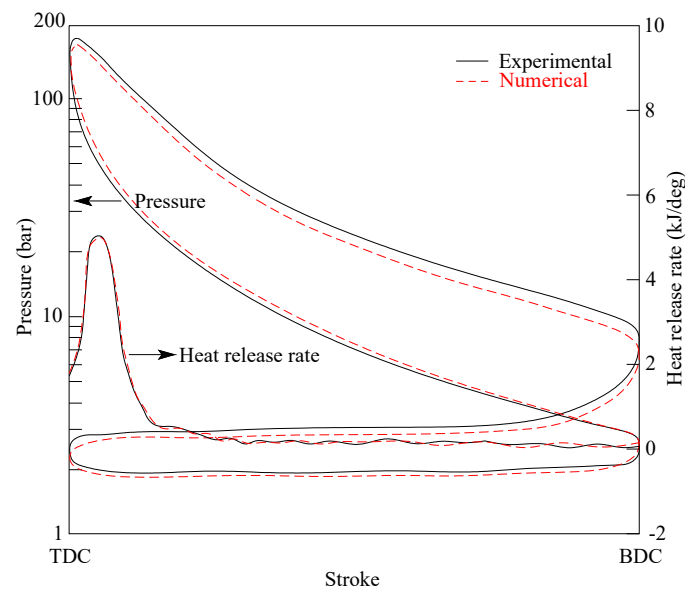


Figure 2. In-cylinder pressure numerically and experimentally obtained, 100% load.

3. Results and Discussion

Once the numerical model was validated with experimental measurements, it was used to analyze the results of several pre-injection patterns. Five pre-injection rates were employed: 5%, 10%, 15%, 20% and 25%; five pre-injection durations: 1° Crank Angle (CA), 2° CA, 3° CA, 4° CA and 5° CA; and five pre-injection starting instants: -22° CA ATDC, -21° CA ATDC, -20° CA ATDC, -19° CA ATDC and -18° CA ATDC. These ranges were chosen according to a previous paper [43], in which it was obtained that wider ranges lead to excessive increments in NO_x emissions or consumption. Taking into account these values of pre-injection rates, durations and starting instants, a total of

125 cases were analyzed. These are summarized in Figure 3. SFC and emissions of NO_x, CO and HC were characterized for these 125 cases.

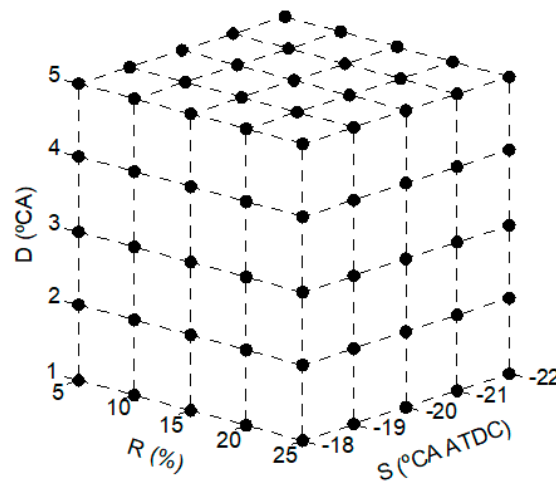


Figure 3. Schematic representation of the cases analyzed.

As indicated previously, a MCDM method was employed. The first step in MCDM approaches consists on defining the decision tree with the relative importance of each parameter, Table 1. Two requirements (general aspects) were considered: consumption and emissions. The second level represents the sub-requirements (specific aspects). The relative importance of each requirement and sub-requirement must be defined too. In the present work, this importance was distributed equally, i.e., the same importance was given to SFC and emissions: 50% ($\alpha = 0.5$ in per unit basis) for each one. Regarding emissions, the same importance was given to NO_x, CO and HC: 33.3% ($\beta = 0.333$ in per unit basis) for each one. It is worth mentioning that other scenarios could also be possible in case it is necessary to provide other levels of importance.

Table 1. Decision tree for the MCDM approach.

Requirement	Sub-Requirement
SFC (50%)	SFC (100%)
Emissions (50%)	NO _x (33.3%)
	CO (33.3%)
	HC (33.3%)

The next step was to calculate the variation of each sub-requirement respect to the case without pre-injection, in per unit basis, Equation (1).

$$V_i = \frac{X_i - X_{ref}}{X_{ref}} \tag{1}$$

where X_i is the value of the sub-requirement i and X_{ref} the value corresponding to the case without pre-injection, i.e., SFC = 172 g/kWh, NO_x = 13.3 g/kWh, CO = 4.5 g/kWh and HC = 5.5 g/kWh. Once each indicator was transformed into its variation in per unit basis, the global adequacy index, AI , was computed by Equation (2).

$$AI = \sum_{i=1}^{125} \alpha_i \beta_i V_i \tag{2}$$

where α_i is the weight of each requirement and β_i the weight of each sub-requirement in per unit basis.

The minimum value of the AI is the most adequate solution. It was determined using an in-house code programmed using the open software GNU Octave. For the parameters analyzed in the present

work, the minimum AI is -0.0122 , corresponding to -19° CA ATDC pre-injection starting instant, 20% pre-injection rate and 1° CA pre-injection duration. The results are detailed in Appendix A. As can be seen in this appendix, the minimum AI value was obtained in the ninety-first case analyzed. On a per-unit basis, SFC varies by 0.067; NO_x -0.3467 , CO 0.0347 and HC 0.0383, corresponding to an SFC increment of SFC 6.7%; NO_x reduction of 34.7%, CO increment of 3.47% and HC increment of 3.83% in comparison with the case without pre-injection. Despite the increments in SFC, CO and HC, these solution results are the most appropriate because the increments are low and the NO_x reduction is too significant.

The results shown in Appendix A indicate that the influence of CO and HC in the AI is not too important due to the low variation of these emissions with the pre-injection rate, duration and starting instant. On the other hand, SFC and NO_x emissions are more sensitive. A representative quantity of pre-injection is necessary, specifically 20%, due to the important reduction on NO_x emissions. Nevertheless, if this pre-injection rate is increased, it leads to important increments in SFC and, to a lesser extent, CO and HC emissions. Regarding the pre-injection instant, early pre-injections are appropriate to reduce NO_x but the increase increment in SFC is considerable; for this reason, a -19° CA ATDC was obtained. Finally, the injection duration mainly affects to NO_x and short injections lead to considerable NO_x reductions. The goal of NO_x reduction using pre-injections is to control the combustion temperature. It is well known that high combustion temperatures promote NO_x formation [56]. In order to control the combustion temperature, it is necessary to rigorously inject the fuel at the optimum instant. It is worth mentioning that in practical applications it is not possible to reduce the injection duration at the desirable level. For instance, the present engine is a four-stroke medium-speed model which runs at 500 rpm, which corresponds to 0.00033 s to reach 1° CA. Some current piezo-injectors are able to switch on and off in tens of microseconds but solenoid or electromagnetic injectors have longer response times. For this reason, pre-injections shorter than 1° CA were not analyzed in the present work. Using 1° CA pre-injection duration, the AI is represented in Figure 4. As can be seen, the minimum value of AI , -0.0122 is reached using 20% pre-injection rate and -19° CA ATDC pre-injection starting instant, as indicated above.

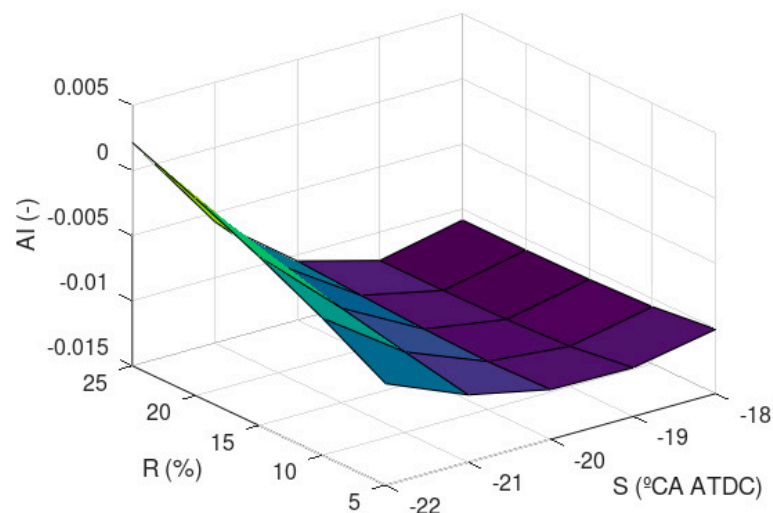


Figure 4. AI against R and S . Pre-injection duration 1° CA.

The consumption against the pre-injection rate and starting instant is shown in Figure 5. This figure refers to 1° CA pre-injection duration. As can be seen, early pre-injections promote considerable increase increments in SFC, as indicated above. On the other hand, the pre-injection rate also promotes increase increments in SFC considerably.

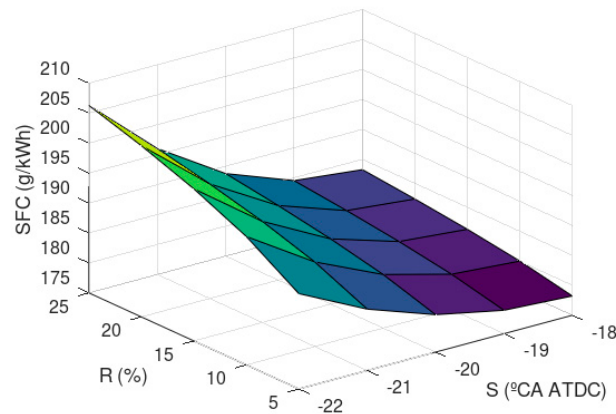


Figure 5. SFC against R and S. Pre-injection duration 1° CA.

NO_x emissions against the pre-injection rate and starting instant are indicated in Figure 6. This figure refers to 1° CA pre-injection duration. As can be seen, early pre-injections promote reductions in NO_x, but increment SFC, as indicated above. On the other hand, the pre-injection rate considerably reduces NO_x but also increments SFC.

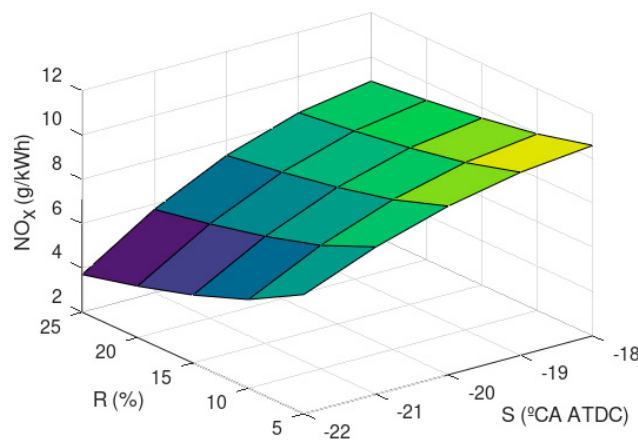


Figure 6. NO_x against R and S. Pre-injection duration 1° CA.

Figures 7 and 8 show the CO and HC emissions against the pre-injection rate and starting instant. These figures refer to 1° CA pre-injection duration. As can be seen, both CO and HC are sensitive to the pre-injection rate and starting instant. Nevertheless, the influence of CO and HC in the results is low due to their low variation.

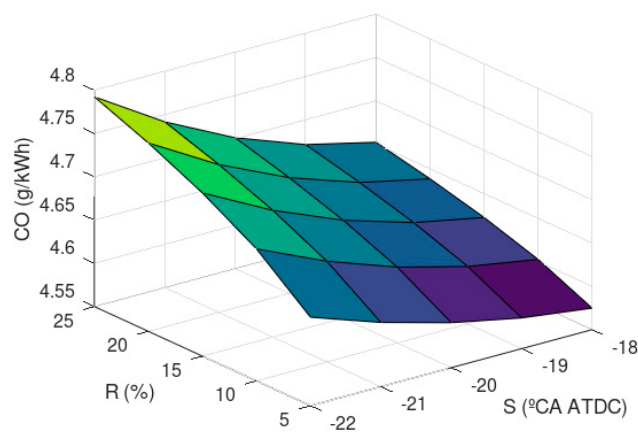


Figure 7. CO against R and S. Pre-injection duration 1° CA.

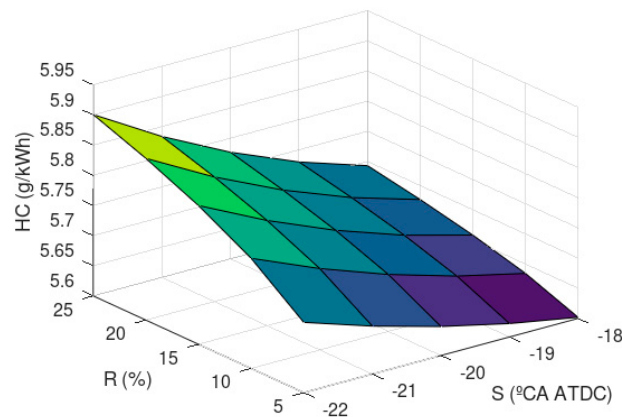


Figure 8. HC against R and S. Pre-injection duration 1° CA.

4. Conclusions

The present work proposes a numerical model to analyze the commercial diesel engine Wärtsilä 6 L 46. Once validated, the numerical model was employed to analyze 125 injection patterns with different values of pre-injection rate, duration and starting instant in the ranges 5% to 25%, 1° CA to 5° CA and −22° CA ATDC to −18° CA ATDC, respectively. Due to this large number of results and the fact that these parameters can lead to different and opposite effects, it is difficult to determine the most adequate injection pattern. According to this, a MCDM approach was employed to select the most appropriate injection pattern. The effects on consumption and emissions of NO_x, CO and HC were characterized. It was found that the injection duration must remain as lower as possible due to significant reductions in NO_x. The most appropriate injection pattern was shown in the 1° CA pre-injection duration, 20% pre-injection rate and −19° CA ATDC pre-injection starting instant. This injection pattern leads to increases in 6.7% in SFC, 3.47% in CO and 3.83% in HC but reduces NO_x by 34.67% in comparison with the case without pre-injection. Future works will focus on analyzing other parameters such as number of pre-injections, dwelling time and injection angle, as well as other engines.

Author Contributions: Conceptualization, M.I.L.G. and C.G.R.V.; methodology, M.I.L.G. and C.G.R.V.; software, M.I.L.G. and C.G.R.V.; validation, M.I.L.G. and C.G.R.V.; formal analysis, M.I.L.G. and L.C.-S.; investigation, M.I.L.G. and C.G.R.V.; resources, M.I.L.G. and C.G.R.V.; writing—original draft preparation, M.I.L.G. and L.C.-S.; writing—review and editing, M.I.L.G. and L.C.-S. All authors have read and agreed to the published version of the manuscript.

Funding: This research received no external funding.

Acknowledgments: The authors would like to express their gratitude to Norplan Engineering S.L. and recommend the courses “CFD with OpenFOAM” and “C ++ applied to OpenFOAM” available at www.technicalcourses.net.

Conflicts of Interest: The authors declare no conflict of interest.

Appendix A

Table A1 lists the results of the 125 cases analyzed by the MCDM approach developed in the present work. Five pre-injection starting instants are included: −22° CA ATDC (Crank Angle After Top Dead Center), −21° CA ATDC, −20° CA ATDC, −19° CA ATDC, and −18° CA ATDC; five pre-injection rates: 5%, 10%, 15%, 20%, and 25%; and five pre-injection durations: 1° CA (Crank Angle), 2° CA, 3° CA, 4° CA, and 5° CA. Table A1 also includes the variation of SFC, NO_x, CO and HC in per unit basis, as well as the AI obtained for each case analyzed. The minimum AI, which represents the most adequate solution, is highlighted. As can be seen, this minimum value was obtained for the 91th case, corresponding to −19° CA ATDC pre-injection starting instant, 20% pre-injection rate, and 1° CA pre-injection duration, leading to variations of 0.067 in SFC, −0.3467 in NO_x, 0.0347 in CO and 0.0383

in HC. In a per cent basis, these values correspond to a SFC increment of 6.7%, NO_x reduction of 34.7%, CO increment of 3.47%, and HC increment of 3.83% in comparison with the case without pre-injection.

Table A1. Results of the 125 cases analyzed.

Case	S (°CA ATDC)	R (%)	D (°CA)	SFC (-)	NO _x (-)	CO (-)	HC (-)	AI (-)
1	-22	5	1	0.1099	-0.4455	0.0338	0.0393	-0.0072
2	-22	5	2	0.0987	-0.4111	0.0385	0.0426	-0.0058
3	-22	5	3	0.0902	-0.3846	0.0446	0.0474	-0.0037
4	-22	5	4	0.0846	-0.3659	0.0523	0.0538	-0.0011
5	-22	5	5	0.0818	-0.3551	0.0613	0.0619	0.0022
6	-22	10	1	0.1421	-0.5484	0.0450	0.0514	-0.0045
7	-22	10	2	0.1275	-0.5061	0.0510	0.0555	-0.0030
8	-22	10	3	0.1166	-0.4735	0.0590	0.0618	-0.0006
9	-22	10	4	0.1094	-0.4505	0.0688	0.0701	0.0027
10	-22	10	5	0.1058	-0.4371	0.0806	0.0805	0.0068
11	-22	15	1	0.1650	-0.6194	0.0530	0.0600	-0.0020
12	-22	15	2	0.1481	-0.5716	0.0600	0.0648	-0.0005
13	-22	15	3	0.1355	-0.5347	0.0693	0.0721	0.0020
14	-22	15	4	0.1271	-0.5087	0.0807	0.0817	0.0057
15	-22	15	5	0.1229	-0.4937	0.0943	0.0938	0.0104
16	-22	20	1	0.1836	-0.6752	0.0595	0.0669	0.0001
17	-22	20	2	0.1648	-0.6231	0.0673	0.0723	0.0016
18	-22	20	3	0.1507	-0.5829	0.0775	0.0804	0.0044
19	-22	20	4	0.1413	-0.5546	0.0902	0.0911	0.0083
20	-22	20	5	0.1367	-0.5382	0.1054	0.1045	0.0135
21	-22	25	1	0.1994	-0.7219	0.0650	0.0728	0.0021
22	-22	25	2	0.1790	-0.6662	0.0734	0.0787	0.0036
23	-22	25	3	0.1637	-0.6232	0.0846	0.0874	0.0065
24	-22	25	4	0.1535	-0.5930	0.0984	0.0991	0.0107
25	-22	25	5	0.1485	-0.5755	0.1149	0.1137	0.0163
26	-21	5	1	0.0770	-0.3497	0.0276	0.0326	-0.0098
27	-21	5	2	0.0658	-0.3153	0.0323	0.0358	-0.0084
28	-21	5	3	0.0573	-0.2888	0.0384	0.0407	-0.0064
29	-21	5	4	0.0517	-0.2701	0.0460	0.0471	-0.0037
30	-21	5	5	0.0489	-0.2593	0.0551	0.0551	-0.0004
31	-21	10	1	0.0995	-0.4305	0.0370	0.0427	-0.0088
32	-21	10	2	0.0850	-0.3882	0.0430	0.0469	-0.0073
33	-21	10	3	0.0741	-0.3555	0.0509	0.0531	-0.0050
34	-21	10	4	0.0668	-0.3325	0.0608	0.0614	-0.0017
35	-21	10	5	0.0633	-0.3192	0.0725	0.0718	0.0024
36	-21	15	1	0.1156	-0.4862	0.0437	0.0499	-0.0077
37	-21	15	2	0.0987	-0.4384	0.0507	0.0547	-0.0062
38	-21	15	3	0.0861	-0.4015	0.0599	0.0620	-0.0037
39	-21	15	4	0.0777	-0.3755	0.0713	0.0716	0.0000
40	-21	15	5	0.0735	-0.3605	0.0850	0.0837	0.0047
41	-21	20	1	0.1286	-0.5300	0.0491	0.0557	-0.0067
42	-21	20	2	0.1098	-0.4779	0.0569	0.0611	-0.0052
43	-21	20	3	0.0957	-0.4377	0.0671	0.0691	-0.0025
44	-21	20	4	0.0864	-0.4094	0.0798	0.0799	0.0015
45	-21	20	5	0.0817	-0.3930	0.0950	0.0933	0.0067
46	-21	25	1	0.1397	-0.5667	0.0537	0.0607	-0.0057
47	-21	25	2	0.1193	-0.5110	0.0621	0.0665	-0.0042
48	-21	25	3	0.1040	-0.4680	0.0733	0.0753	-0.0014
49	-21	25	4	0.0938	-0.4377	0.0871	0.0869	0.0029
50	-21	25	5	0.0888	-0.4202	0.1036	0.1015	0.0085
51	-20	5	1	0.0537	-0.2774	0.0227	0.0269	-0.0112
52	-20	5	2	0.0425	-0.2431	0.0273	0.0301	-0.0098
53	-20	5	3	0.0341	-0.2165	0.0335	0.0350	-0.0077
54	-20	5	4	0.0285	-0.1979	0.0411	0.0414	-0.0050
55	-20	5	5	0.0257	-0.1870	0.0502	0.0494	-0.0018
56	-20	10	1	0.0695	-0.3416	0.0306	0.0353	-0.0113
57	-20	10	2	0.0549	-0.2992	0.0366	0.0395	-0.0098
58	-20	10	3	0.0440	-0.2666	0.0445	0.0457	-0.0074
59	-20	10	4	0.0368	-0.2436	0.0544	0.0540	-0.0042
60	-20	10	5	0.0332	-0.2303	0.0661	0.0644	-0.0001
61	-20	15	1	0.0807	-0.3857	0.0362	0.0413	-0.0111
62	-20	15	2	0.0638	-0.3379	0.0432	0.0462	-0.0096
63	-20	15	3	0.0511	-0.3011	0.0525	0.0534	-0.0070
64	-20	15	4	0.0427	-0.2751	0.0639	0.0631	-0.0034
65	-20	15	5	0.0386	-0.2601	0.0775	0.0751	0.0013
66	-20	20	1	0.0898	-0.4205	0.0408	0.0462	-0.0108

Table A1. Cont.

Case	S (°CA ATDC)	R (%)	D (°CA)	SFC (–)	NO _x (–)	CO (–)	HC (–)	AI (–)
67	–20	20	2	0.0710	–0.3684	0.0486	0.0516	–0.0093
68	–20	20	3	0.0569	–0.3282	0.0589	0.0596	–0.0066
69	–20	20	4	0.0475	–0.2999	0.0716	0.0704	–0.0026
70	–20	20	5	0.0429	–0.2835	0.0868	0.0838	0.0026
71	–20	25	1	0.0975	–0.4496	0.0447	0.0503	–0.0105
72	–20	25	2	0.0771	–0.3939	0.0532	0.0561	–0.0090
73	–20	25	3	0.0618	–0.3509	0.0643	0.0649	–0.0061
74	–20	25	4	0.0516	–0.3207	0.0781	0.0766	–0.0019
75	–20	25	5	0.0466	–0.3031	0.0946	0.0911	0.0037
76	–19	5	1	0.0401	–0.2287	0.0190	0.0222	–0.0113
77	–19	5	2	0.0289	–0.1944	0.0237	0.0254	–0.0098
78	–19	5	3	0.0204	–0.1678	0.0298	0.0303	–0.0078
79	–19	5	4	0.0148	–0.1492	0.0374	0.0367	–0.0051
80	–19	5	5	0.0121	–0.1384	0.0465	0.0447	–0.0018
81	–19	10	1	0.0519	–0.2816	0.0258	0.0292	–0.0119
82	–19	10	2	0.0373	–0.2393	0.0319	0.0334	–0.0104
83	–19	10	3	0.0264	–0.2066	0.0398	0.0396	–0.0080
84	–19	10	4	0.0192	–0.1837	0.0497	0.0479	–0.0048
85	–19	10	5	0.0156	–0.1703	0.0614	0.0583	–0.0007
86	–19	15	1	0.0602	–0.3180	0.0308	0.0343	–0.0121
87	–19	15	2	0.0433	–0.2703	0.0378	0.0391	–0.0106
88	–19	15	3	0.0307	–0.2334	0.0470	0.0463	–0.0080
89	–19	15	4	0.0223	–0.2074	0.0584	0.0560	–0.0044
90	–19	15	5	0.0181	–0.1924	0.0721	0.0681	0.0003
91	–19	20	1	0.0670	–0.3467	0.0347	0.0383	–0.0122
92	–19	20	2	0.0482	–0.2946	0.0425	0.0437	–0.0107
93	–19	20	3	0.0341	–0.2544	0.0528	0.0518	–0.0080
94	–19	20	4	0.0248	–0.2261	0.0655	0.0625	–0.0040
95	–19	20	5	0.0201	–0.2097	0.0807	0.0759	0.0012
96	–19	25	1	0.0728	–0.3707	0.0381	0.0418	–0.0122
97	–19	25	2	0.0524	–0.3150	0.0465	0.0476	–0.0107
98	–19	25	3	0.0371	–0.2720	0.0577	0.0564	–0.0079
99	–19	25	4	0.0269	–0.2418	0.0715	0.0680	–0.0036
100	–19	25	5	0.0219	–0.2242	0.0880	0.0826	0.0020
101	–18	5	1	0.0361	–0.2036	0.0166	0.0185	–0.0101
102	–18	5	2	0.0249	–0.1692	0.0213	0.0217	–0.0086
103	–18	5	3	0.0164	–0.1427	0.0274	0.0266	–0.0066
104	–18	5	4	0.0108	–0.1241	0.0351	0.0330	–0.0039
105	–18	5	5	0.0081	–0.1132	0.0441	0.0410	–0.0007
106	–18	10	1	0.0467	–0.2507	0.0228	0.0245	–0.0106
107	–18	10	2	0.0322	–0.2084	0.0288	0.0286	–0.0091
108	–18	10	3	0.0213	–0.1757	0.0368	0.0349	–0.0068
109	–18	10	4	0.0140	–0.1527	0.0466	0.0432	–0.0035
110	–18	10	5	0.0104	–0.1394	0.0583	0.0536	0.0006
111	–18	15	1	0.0543	–0.2831	0.0272	0.0287	–0.0108
112	–18	15	2	0.0374	–0.2353	0.0342	0.0336	–0.0093
113	–18	15	3	0.0247	–0.1984	0.0434	0.0408	–0.0067
114	–18	15	4	0.0163	–0.1725	0.0549	0.0505	–0.0031
115	–18	15	5	0.0121	–0.1574	0.0685	0.0625	0.0016
116	–18	20	1	0.0604	–0.3086	0.0308	0.0322	–0.0109
117	–18	20	2	0.0416	–0.2565	0.0386	0.0375	–0.0094
118	–18	20	3	0.0275	–0.2163	0.0488	0.0456	–0.0066
119	–18	20	4	0.0181	–0.1880	0.0615	0.0563	–0.0027
120	–18	20	5	0.0135	–0.1716	0.0767	0.0697	0.0025
121	–18	25	1	0.0656	–0.3300	0.0338	0.0351	–0.0108
122	–18	25	2	0.0451	–0.2743	0.0423	0.0409	–0.0094
123	–18	25	3	0.0298	–0.2313	0.0534	0.0497	–0.0065
124	–18	25	4	0.0197	–0.2010	0.0672	0.0613	–0.0023
125	–18	25	5	0.0146	–0.1835	0.0837	0.0759	0.0033

References

- Shen, H.; Zhang, J.; Yang, B.; Jia, B. Development of a marine two-stroke diesel engine MVEM with in-cylinder pressure predictive capability and a novel compressor model. *J. Mar. Sci. Eng.* **2020**, *8*, 204. [[CrossRef](#)]
- Sencic, T.; Mrzljak, V.; Blecich, P.; Bonfacic, I. 2D CFD simulation of water injection strategies in a large marine engine. *J. Mar. Sci. Eng.* **2019**, *7*, 296. [[CrossRef](#)]

3. Sinay, J.; Puskar, M.; Kopas, M. Reduction of the NO_x emissions in vehicle diesel engine in order to fulfill future rules concerning emissions released into air. *Sci. Total Environ.* **2018**, *624*, 1421–1428. [[CrossRef](#)] [[PubMed](#)]
4. Lamas, M.I.; Rodriguez, C.G. Emissions from marine engines and NO_x reduction methods. *J. Marit. Res.* **2012**, *9*, 77–82.
5. di Sarli, V.; di Benedetto, A. Using CFD simulation as a tool to identify optimal operating conditions for regeneration of a catalytic diesel particulate filter. *Appl. Sci.* **2019**, *9*, 3453. [[CrossRef](#)]
6. Lamas, M.I.; Rodriguez, C.G. NO_x reduction in diesel-hydrogen engines using different strategies of ammonia injection. *Energies* **2019**, *12*, 1255. [[CrossRef](#)]
7. Lamas, M.I.; Rodriguez, C.G. Numerical model to analyze NO_x reduction by ammonia injection in diesel-hydrogen engines. *Int. J. Hydrog. Energy* **2017**, *42*, 26132–26141. [[CrossRef](#)]
8. Leach, F.; Ismail, R.; Davy, M. Engine-out emissions from a modern high speed diesel engine—The importance of nozzle tip protrusion. *Appl. Energy* **2018**, *226*, 340–352. [[CrossRef](#)]
9. Gao, Z.; Schreiber, W. The effects of EGR and split fuel injection on diesel engine emission. *Int. J. Automot. Technol.* **2001**, *2*, 123–133.
10. Park, S.W.; Suh, H.K.; Lee, C.S. Effects of a split injection on spray characteristics for a common-rail type diesel injection system. *Int. J. Automot. Technol.* **2005**, *6*, 315–322.
11. Chen, S.K. *Simultaneous Reduction of NO_x and Particulate Emissions by Using Multiple Injections in a Small Diesel Engine*; SAE Technical Paper 2000-01-3084; SAE International: Warrendale, PA, USA, 2000. [[CrossRef](#)]
12. Shundoh, S.; Komori, M.; Tsujimura, K.; Kobayashi, S. *NO_x Reduction from Diesel Combustion Using Pilot Injection with High Pressure Fuel Injection*; SAE Technical Paper 920461; SAE International: Warrendale, PA, USA, 1992. [[CrossRef](#)]
13. Carlucci, P.; Ficarella, A.; Laforgia, D. *Effects of Pilot Injection Parameters on Combustion for Common Rail Diesel Engines*; SAE Technical Paper 2003-01-0700; SAE International: Warrendale, PA, USA, 2003. [[CrossRef](#)]
14. Tanaka, T.; Ando, A.; Ishizaka, K. Study on pilot injection of DI diesel engine using common rail injection system. *JSAE Rev.* **2002**, *23*, 297–302. [[CrossRef](#)]
15. Benajes, J.; Molina, S.; Novella, R.; DeRudder, K. Influence of injection conditions and exhaust gas recirculation in a high-speed direct-injection diesel engine operating with a late split injection. *Proc. Inst. Mech. Eng. Part D: J. Automob. Eng.* **2008**, *222*, 629–641. [[CrossRef](#)]
16. Pierpont, D.; Montgomery, D.; Reitz, R. *Reducing Particulate and NO_x Using Multiple Injections and EGR in a DI Diesel*; SAE Technical Paper 950217; SAE International: Warrendale, PA, USA, 1995. [[CrossRef](#)]
17. Hotta, Y.; Inayoshi, M.; Nakakita, K.; Fujiwara, K. *Achieving Lower Exhaust Emissions and Better Performance in an HSDI Diesel Engine with Multiple Injection*; SAE Technical Paper 2005-01-0928; SAE International: Warrendale, PA, USA, 2005. [[CrossRef](#)]
18. Fang, T.; Coverdill, R.; Lee, C.F.; White, R.A. Effects of injection angles on combustion process using multiple injection strategies in an HSDI diesel engine. *Fuel* **2008**, *87*, 3232–3239. [[CrossRef](#)]
19. Ishida, M.; Chen, Z.L.; Luo, G.F.; Ueki, H. *The Effect of Pilot Injection on Combustion in a Turbocharged D. I. Diesel Engine*; SAE Technical Paper 941692; SAE International: Warrendale, PA, USA, 1994. [[CrossRef](#)]
20. Minami, T.; Takeuchi, K.; Shimazaki, N. *Reduction of Diesel Engine NO_x Using Pilot Injection*; SAE Technical Paper 950611; SAE International: Warrendale, PA, USA, 1995. [[CrossRef](#)]
21. Dhar, A.; Agarwal, A.K. Experimental investigations of the effect of pilot injection on performance, emissions and combustion characteristics of Karanja biodiesel fuelled CRDI engine. *Energy Convers. Manag.* **2015**, *93*, 357–366. [[CrossRef](#)]
22. Puskar, M.; Bigos, P. Output performance increase of two-stroke combustion engine with detonation combustion optimization. *Strojarsstvo* **2010**, *52*, 577–587.
23. Puskar, M.; Brestovic, T.; Jasminska, N. Numerical simulation and experimental analysis of acoustic wave influences on brake mean effective pressure in thrust-ejector inlet pipe of combustion engine. *Int. J. Veh. Des.* **2015**, *67*, 63–76. [[CrossRef](#)]
24. Hunicz, J.; Geca, M.S.; Kordos, P.; Komsta, H. An experimental study on a boosted gasoline HCCI engine under different direct fuel injection strategies. *Exp. Therm. Fluid Sci.* **2015**, *62*, 151–163. [[CrossRef](#)]
25. Alla, G.H.A.; Soliman, H.A.; Badr, O.A. Effect of injection timing on the performance of a dual fuel engine. *Energy Convers. Manag.* **2002**, *43*, 269–277. [[CrossRef](#)]

26. Papagiannakis, R.G.; Hountalas, D.T.; Rakopoulos, C.D. Theoretical study of the effects of pilot fuel quantity and its injection timing on the performance and emissions of a dual fuel diesel engine. *Energy Convers. Manag.* **2007**, *48*, 2951–2961. [[CrossRef](#)]
27. Ryu, K. Effects of pilot injection timing on the combustion and emissions characteristics in a diesel engine using biodiesel–CNG dual fuel. *Appl. Energy* **2013**, *111*, 721–730. [[CrossRef](#)]
28. Yang, B.; Wang, L.; Ning, L.; Zeng, K. Effects of pilot injection timing on the combustion noise and particle emissions of a diesel/natural gas dual-fuel engine at low load. *Appl. Therm. Eng.* **2016**, *102*, 822–828. [[CrossRef](#)]
29. Seddiek, I.S.; Elgohary, M.M.; Ammar, N. The hydrogen-fuelled internal combustion engines for marine applications with a case study. *Brodogradnja* **2015**, *66*, 23–38.
30. Carlucci, A.P.; Ficarella, A.; Laforgia, D. Control of the combustion behaviour in a diesel engine using early injection and gas addition. *Appl. Therm. Eng.* **2006**, *26*, 2279–2286. [[CrossRef](#)]
31. Hwang, J.; Qi, D.; Jung, Y.; Bae, C. Effect of injection parameters on the combustion and emission characteristics in a common-rail direct injection diesel engine fueled with waste cooking oil biodiesel. *Renew. Energy* **2014**, *63*, 9–17. [[CrossRef](#)]
32. Sinay, J.; Tompos, A.; Puskar, M.; Pctkova, V. Multiparametric diagnostics of gas engines. *Trans. R. Inst. Nav. Archit. Part A: Int. J. Marit. Eng.* **2014**, *156*, 149–156. [[CrossRef](#)]
33. Shi, J.; Wang, T.; Zhao, Z.; Yang, T.; Zhang, Z. Experimental study of injection parameters on the performance of a diesel engine with Fischer-Tropsch fuel synthesized from coal. *Energies* **2018**, *11*, 3280. [[CrossRef](#)]
34. di Sarli, V. Stability and emissions of a lean pre-mixed combustor with rich catalytic/lean-burn pilot. *Int. J. Chem. React. Eng.* **2014**, *12*, 77–89. [[CrossRef](#)]
35. Lechner, G.; Jacobs, T.; Chryssakis, C. *Evaluation of a Narrow Spray Cone Angle, Advanced Injection Timing Strategy to Achieve Partially Premixed Compression Ignition Combustion in a Diesel Engine*; SAE Technical Paper 2005-01-0167; SAE International: Warrendale, PA, USA, 2005. [[CrossRef](#)]
36. Sun, Y.; Reitz, R.D. *Modeling Diesel Engine NOx and Soot Reduction with Optimized Two-Stage Combustion*; SAE Technical Paper 2006-01-0027 2006; SAE International: Warrendale, PA, USA, 2006. [[CrossRef](#)]
37. Verbiezen, K.; Donkerbroek, A.J.; Klein-Douwel, R.J.H.; van Vliet, A.P.; Frijters, P.J.M.; Seykens, X.L.J. Diesel combustion: In-cylinder NO concentrations in relation to injection timing. *Combust. Flame* **2007**, *151*, 333–346. [[CrossRef](#)]
38. Zehni, A.; Jafarmadar, S. Multi-dimensional modeling of the effects of split injection scheme on combustion and emissions of direct-injection diesel engines at full load state. *IJE Trans.* **2009**, *22*, 369–378.
39. Abdullah, N.R.; Mamat, R.; Rounce, P.; Tsolakis, A.; Wyszynski, M.L.; Xu, H.M. *Effect of Injection Pressure with Split Injection in a V6 Diesel Engine*; SAE Technical Paper 2009-20-0049; SAE International: Warrendale, PA, USA, 2009; Volume 16, pp. 1–11. [[CrossRef](#)]
40. Coskun, G.; Soyhan, H.S.; Demir, U.; Turkcan, A.; Ozsezen, A.N.; Canakci, M. Influences of second injection variations on combustion and emissions of an HCCI-DI engine: Experiments and CFD modelling. *Fuel* **2014**, *136*, 287–294. [[CrossRef](#)]
41. Wang, X.; Zhao, H.; Xie, H. Effect of piston shapes and fuel injection strategies on stoichiometric stratified flame ignition (SFI) hybrid combustion in a PFI/DI gasoline engine by numerical simulations. *Energy Convers. Manag.* **2015**, *98*, 387–400. [[CrossRef](#)]
42. Zhaojie, S.; Cui, W.; Ju, X.; Liu, Z. Numerical investigation on effects of assigned EGR stratification on a heavy duty diesel engine with two-stage fuel injection. *Energies* **2018**, *11*, 515. [[CrossRef](#)]
43. Lamas, M.I.; de Dios Rodriguez, J.; Castro-Santos, L.; Carral, L.M. Effect of multiple injection strategies on emissions and performance in the Wärtsilä 6L 46 marine engine. A numerical approach. *J. Clean. Prod.* **2019**, *206*, 1–10. [[CrossRef](#)]
44. Lamas, M.I.; Rodriguez, C.G. Computational fluid dynamics analysis of the scavenging process in the MAN B&W 7S50MC two-stroke diesel marine engine. *J. Ship Res.* **2012**, *56*, 154–161. [[CrossRef](#)]
45. Sencic, T. Analysis of soot and NOx emissions reduction possibilities on modern low speed, two-stroke, diesel engines. *Strojarstvo* **2010**, *52*, 525–533.
46. Ricart, L.M.; Xin, J.; Bower, G.R.; Reitz, R.D. *In-Cylinder Measurement and Modeling of Liquid Fuel Spray Penetration in a Heavy-Duty Diesel Engine*; SAE Technical Paper 971591; SAE International: Warrendale, PA, USA, 1997. [[CrossRef](#)]

47. Dukowicz, J.K. A particle-fluid numerical model for liquid sprays. *J. Comput. Phys.* **1980**, *35*, 229–253. [[CrossRef](#)]
48. Ra, Y.; Reitz, R. A reduced chemical kinetic model for IC engine combustion simulations with primary reference fuels. *Combust. Flame* **2008**, *155*, 713–738. [[CrossRef](#)]
49. Yang, H.; Krishnan, S.R.; Srinivasan, K.K.; Midkiff, K.C. Modeling of NO_x emissions using a superextended Zeldovich mechanism. In Proceedings of the ICEF03 2003 Fall Technical Conference of the ASME Internal Combustion Engine Division, Erie, PA, USA, 7–10 September 2003.
50. Miller, J.A.; Glarborg, P. Modeling the formation of N₂O and NO₂ in the thermal DeNO_x process. *Springer Ser. Chem. Phys.* **1996**, *61*, 318–333.
51. Lamas, M.I.; Rodríguez, C.G.; Rebolledo, J.M. Numerical model to study the valve overlap period in the Wärtsilä 6L46 four-stroke marine engine. *Pol. Marit. Res.* **2012**, *1*, 31–37. [[CrossRef](#)]
52. Lamas, M.I.; Rodríguez, C.G. Numerical model to study the combustion process and emissions in the Wärtsilä 6L 46 four-stroke marine engine. *Pol. Marit. Res.* **2013**, *20*, 61–66. [[CrossRef](#)]
53. Galdo, M.I.L.; Castro-Santos, L.; Vidal, C.G.R. Numerical analysis of NO_x reduction using ammonia injection and comparison with water injection. *J. Mar. Sci. Eng.* **2020**, *8*, 109. [[CrossRef](#)]
54. Lamas, M.I.; Rodríguez, C.G.; Telmo, J.; Rodríguez, J.D. Numerical analysis emissions from marine engines using alternative fuels. *Pol. Marit. Res.* **2015**, *22*, 48–52. [[CrossRef](#)]
55. Lamas, M.I.; Rodríguez, C.G.; Rodríguez, J.D.; Telmo, J. Internal modifications to reduce pollutant emissions from marine engines. A numerical approach. *Int. J. Nav. Archit. Mar. Eng.* **2013**, *5*, 493–501. [[CrossRef](#)]
56. Heywood, J. *Internal Combustion Engine Fundamentals*, 2nd ed.; McGraw-Hill Education: New York, NY, USA, 2018.



© 2020 by the authors. Licensee MDPI, Basel, Switzerland. This article is an open access article distributed under the terms and conditions of the Creative Commons Attribution (CC BY) license (<http://creativecommons.org/licenses/by/4.0/>).